

## Sedimentation, bioturbation, and Hg uptake in the sediments of the estuary and Gulf of St. Lawrence

J. N. Smith

Marine Environmental Sciences Division, Bedford Institute of Oceanography, Fisheries and Oceans Canada, Dartmouth, Nova Scotia B2Y 4A2

C. T. Schafer

Geological Survey of Canada, Bedford Institute of Oceanography, Dartmouth, Nova Scotia B2Y 4A2

### Abstract

Sedimentation rates and mixing depths have been estimated from the application of a two-layer biodiffusion model to  $^{210}\text{Pb}$  profiles in sediment cores collected in the Laurentian Trough in the Estuary and Gulf of St. Lawrence. Sedimentation rates decrease exponentially with distance seaward from  $0.70\text{ cm yr}^{-1}$  ( $0.47\text{ g cm}^{-2}\text{ yr}^{-1}$ ) near the head of the Trough to  $0.04\text{ cm yr}^{-1}$  ( $0.03\text{ g cm}^{-2}\text{ yr}^{-1}$ ) in the Gulf of St. Lawrence. Mercury (Hg) sediment profiles exhibit subsurface maxima that decrease from concentrations of  $0.6\text{ }\mu\text{g g}^{-1}$  near the entrance to the Saguenay Fjord to  $0.04\text{ }\mu\text{g g}^{-1}$  in the central part of the Gulf. Hg release data for a chloralkali plant on the Saguenay River were used as the input function for the biodiffusion model and provided accurate simulation of measured profiles when mixing was permitted to extend into the deep ( $>10\text{ cm}$ ) sediment layer. Estimates of Hg sediment inventories indicate that 100–130 tonnes (t) of Hg have been retained within the sediments of the St. Lawrence Estuary, which, combined with an Hg inventory of 30 t estimated for the sediments of the Saguenay Fjord, approximately balance the 136 t of Hg released from the chloralkali plant since 1947.  $^{137}\text{Cs}$  and  $^{239,240}\text{Pu}$  sediment-depth profiles were also simulated by the biodiffusion model using input functions based on atmospheric fallout modified by radionuclide transport through the St. Lawrence River drainage basin.

During the early 1970s, fish and crustaceans in the Saguenay Fjord in Eastern Quebec were found to be severely contaminated by mercury, resulting in the closure of local fisheries. Geochronologies measured using  $^{210}\text{Pb}$  (Smith and Walton 1980) and fallout radionuclides ( $^{137}\text{Cs}$ ,  $^{239,240}\text{Pu}$ ; Smith and Ellis 1982) in Hg-contaminated sediments indicated that the date ( $1947 \pm 3$ ) for the initial contamination by Hg was synchronous with the construction of a chloralkali plant at Arvida on the Saguenay River (Smith and Loring 1981; Smith 1988). These and later studies (reviewed in Cossa 1990) confirmed that the source of the Hg pollution was the chloralkali plant, which, during its lifetime, released at least 136 tonnes of Hg into the environment prior to its eventual closure in 1976 (Smith and Loring 1981). An important question arising from these earlier studies is, to what extent have St. Lawrence Estuary sediments been contaminated by the same Hg source. This issue has commercial implications because the Estuary and Gulf of St. Lawrence collectively support a large fishery that is vulnerable to toxic chemical contamination through the food web (Gagnon et al. 1996), as evidenced by the closing of large areas to shellfish harvesting (Masse et al. 1986; Gagne and Sinclair 1991). The purpose of the present study was: (1) to determine sedimentation and mixing rates in the sediments of the Lauren-

tian Trough using radionuclide ( $^{210}\text{Pb}$ ,  $^{137}\text{Cs}$ , and  $^{239,240}\text{Pu}$ ) tracers, and (2) to utilize these data, together with measurements of Hg concentrations, in a biodiffusion model to determine the magnitude and timing of Hg contamination of the St. Lawrence Estuary.

### Materials and methods

*Field and laboratory*—A suite of box and Lehigh gravity cores was collected along the longitudinal axis of the Laurentian Channel in 1987 at stations indicated in Fig. 1. Hg and radionuclide data are also reported for a gravity core (D-1) collected at the head of the Saguenay Fjord in 1979 (Smith et al. 1987). Box cores were subsampled at 1-cm intervals aboard the vessel, and the gravity cores were stored upright at  $4^\circ\text{C}$  and subsequently x-radiographed and subsampled at the BIO laboratory.  $^{210}\text{Pb}$  was determined on freeze-dried sediment samples by alpha counting of  $^{210}\text{Po}$  electro-deposited onto nickel disks, while the  $^{226}\text{Ra}$ -supported  $^{210}\text{Pb}$  levels were determined on acid-digested sediment samples using a radon gas emanation method.  $^{137}\text{Cs}$  was measured on dried sediment samples using a hyperpure Ge gamma ray detector having a 1-cm-diameter well.  $^{239,240}\text{Pu}$  was measured through initial radiochemical separation using ion-exchange techniques, followed by electrodeposition onto platinum electrodes and subsequent analysis by alpha particle spectrometry (Smith et al. 1987).

Sediment subsamples used for Hg and organic carbon analyses were air dried and stored in airtight bottles. Hg was determined in duplicate for each sample by initial digestion and oxidation of the sediment sample in concentrated  $\text{HNO}_3$  and  $\text{H}_2\text{SO}_4$  and followed by reduction of Hg to its elemental

### Acknowledgments

The authors thank G. Folwarcznay for undertaking the Hg and radionuclide analyses and the crew and officers of the CSS *Dawson*. We are also grateful to B. Boudreau (Dalhousie University, Halifax, Nova Scotia), who provided the code for the biodiffusion model, and to J. Syvitski and D. Buckley (formerly, Geological Survey of Canada, BIO) for critical reviews of the manuscript.

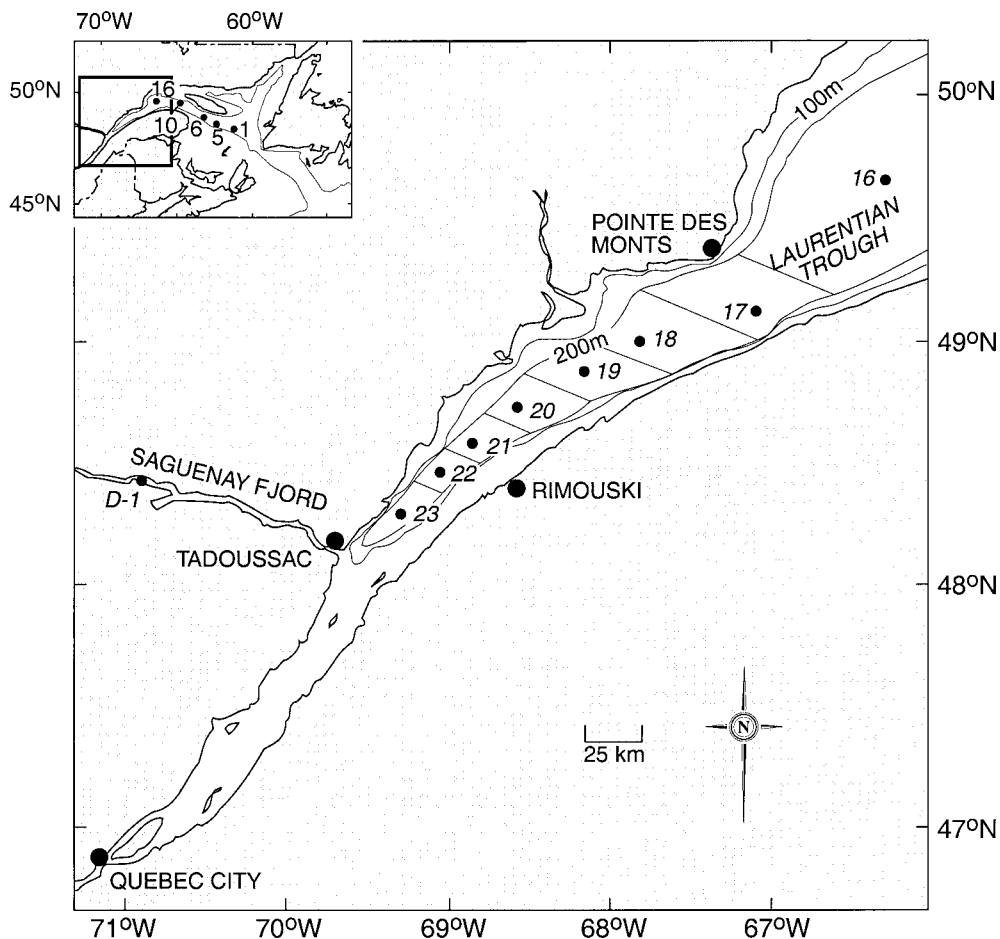


Fig. 1. Station locations for sediment cores collected in the Laurentian Trough of the Estuary and Gulf of St. Lawrence and Sta. D-1 in the Saguenay Fjord.

state with stannous chloride. Analyses were performed using flameless atomic absorption procedures (Loring and Rantala 1992). Replicate analyses (eight) of a sample with an average of  $0.210 \mu\text{g g}^{-1}$  gave a standard deviation of  $\pm 0.025 \mu\text{g g}^{-1}$ , for a coefficient of variation of 11.9%. An accuracy of 3% for the analyses was determined using the certified reference material, NRCC Marine Sediment BEST-1 ( $0.092 \pm 0.009 \mu\text{g g}^{-1}$  Hg). The detection limit is  $0.008 \mu\text{g g}^{-1}$ . Readily oxidizable organic matter was determined by the wet oxidation method (cold  $\text{H}_2\text{SO}_4$ ) described by Loring and Rantala (1992). Textural analyses were determined using standard sieving and sedigraph techniques. Detailed porosity profiles were determined for each core and used to determine the integrated mass of dry sediment (mass depth;  $\text{g cm}^{-2}$ ) above each depth (cm) horizon.

*Environmental setting*—The morphology of the St. Lawrence Estuary is marked by a deep submarine valley referred to as the Laurentian Trough, which is flanked by submarine platforms and shelves of varying width and relief (Fig. 1). The Trough begins near the mouth of the Saguenay River and follows an easterly direction through the Gulf of St. Lawrence to its terminus at a depth of between 500 and 600 m at the edge of the continental shelf (Fig. 1). It has

steep walls and a broad hummocky floor separated into a series of basins having water depths in excess of 250–300 m. These water depths permit the penetration of relatively unmodified North Atlantic water for a distance of 1,200 km into the North American land mass, resulting in the extension of a continental shelf oceanographic environment to the head of the Estuary.

The St. Lawrence Estuary is considered to be divided into “Upper” and “Lower” sections, with a boundary positioned near the mouth of the Saguenay Fjord (Therriault et al. 1990). The Lower Estuary undergoes a transition from two-layer estuarine circulation near the mouth of the Saguenay Fjord to more oceanic circulation patterns typical of shelf environments in the Gulf of St. Lawrence (Strain 1988). With a major portion of North America as its drainage basin, the St. Lawrence River delivers a mean freshwater discharge of  $12,000 \text{ m}^3 \text{ s}^{-1}$ , close to that of the Mississippi River. However, because of the trapping of suspended solids in the Great Lakes basins, the suspended matter discharge of the St. Lawrence is two orders of magnitude less than that of the Mississippi. Sediment texture shifts from sands and silts deposited under the more energetic estuarine conditions prevailing at the head of the Trough to clay-sized material de-

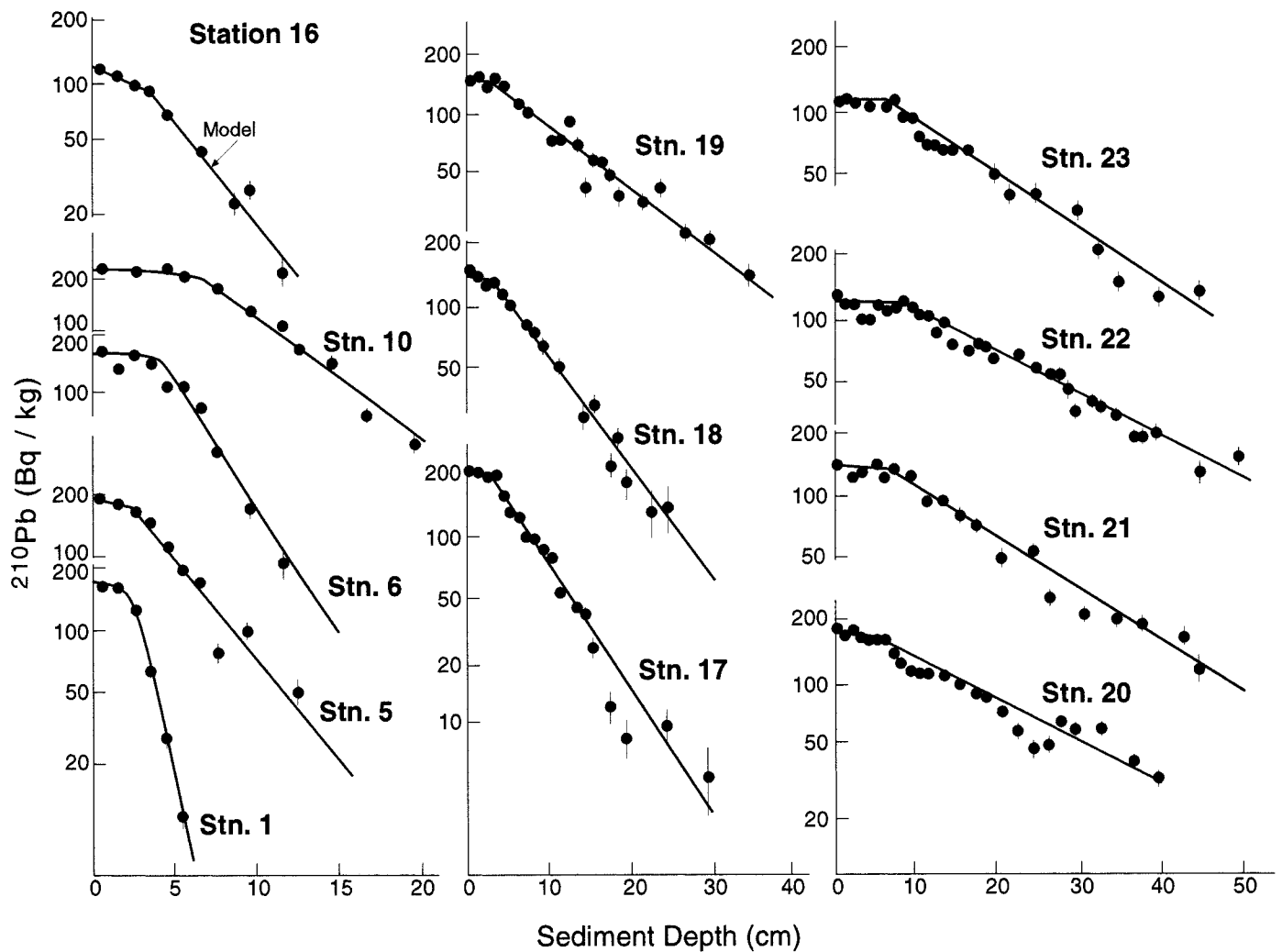


Fig. 2. Excess  $^{210}\text{Pb}$  ( $\text{Bq kg}^{-1}$ ) vs. depth (cm) for Laurentian Trough sediment cores. Solid lines represent steady-state results of two-layer biodiffusion model for values of  $\omega$  and  $L$  given in Table 1. Mixing is confined to the SML, i.e.,  $D_b^0 = 10 \text{ cm}^2 \text{ yr}^{-1}$ ,  $D_b^z = 0$ .

posited in the lower energy distal reaches of the Estuary (Loring and Nota 1973; Loring 1988).

## Results and discussion

**$^{210}\text{Pb}/^{226}\text{Ra}$  results**—Excess  $^{210}\text{Pb}$  activities (equal to the total  $^{210}\text{Pb}$  activity minus the background  $^{226}\text{Ra}$  activity) for the Laurentian Trough sediment cores are plotted on a semi-logarithmic scale as a function of sediment depth (cm) in Fig. 2. The  $^{226}\text{Ra}$  activity increases from a value of  $13 \text{ Bq kg}^{-1}$  in the more silty sediments at Sta. 23 near the headwall of the Trough to a value of  $33 \text{ Bq kg}^{-1}$  in the predominantly clay-sized sediments (Loring and Nota 1973) at Sta. 1 in the center of the Gulf of St. Lawrence. A similar, inverse dependence of  $^{226}\text{Ra}$  activity on particle size was observed in the Saguenay Fjord (Smith and Walton 1980) and was shown to reflect the higher concentrations of  $^{226}\text{Ra}$  associated with the clay component of muddy sediments.

**Biodiffusion model**— $^{210}\text{Pb}$  distributions in the cores are characterized by an upper surface mixed layer (SML) with

a reduced  $^{210}\text{Pb}$  activity gradient, overlying sediments in which the  $^{210}\text{Pb}$  activity decreases exponentially as a function of depth. In accordance with previous interpretations of this commonly observed feature in lake and marine deposits (Robbins and Edgington 1975; Olsen et al. 1981; Carpenter et al. 1982), sediments in the SML are assumed to have undergone mixing as a consequence of the feeding and burrowing activities of small, epifaunal organisms, while the lower zone is assumed to represent a region of negligible or reduced mixing attributable to deeper burrowing infaunal species. The infauna of the Laurentian Trough sediments are dominated by tube-building polychaete worms (Silverberg and Sundby 1990; White 1994), and these tubes are evident in x-radiographs of the cores. Deep burrowing is indicated by the preservation of tubes below depths of 10–15 cm in cores from the Lower Estuary.

When sediment reworking by organisms promotes the random movement of particles over short distances (local mixing), bioturbation can be simulated by the classical diffusion equation, with the complex processes governing mixing being parameterized in a single factor, the biodiffusion coef-

Table 1. Sedimentation rates ( $\omega$ ), mass accumulation rates ( $\omega_m$ ), mixing depths ( $L$ ), radionuclide inventories, and inventory ratios for Lower Estuary (Sta. 17–23) and Gulf of St. Lawrence (Sta. 1–16) cores. Core D-1 (Saguenay Fjord) and atmospheric fallout results (to 1987) are summarized at bottom of table (Smith et al. 1987).

Sta.	Area (km <sup>2</sup> )	$\omega$ (cm yr <sup>-1</sup> )	$\omega_m$ (g cm <sup>-2</sup> yr <sup>-1</sup> )	$L$ (cm)	<sup>210</sup> Pb inventory (Bq cm <sup>-2</sup> )	Hg inventory ( $\mu$ g cm <sup>-2</sup> )	<sup>137</sup> Cs inventory (mBq cm <sup>-2</sup> )	<sup>239,240</sup> Pu inventory (mBq cm <sup>-2</sup> )	$\frac{^{137}\text{Cs}}{^{239,240}\text{Pu}}$	$\frac{^{210}\text{Pb}}{^{239,240}\text{Pu}}$
1	—	0.042	0.031	2	0.30	0.00	7.67	1.83	4.18	165
5	—	0.150	0.063	2	0.49	0.00	12.5	3.00	4.17	163
6	—	0.115	0.060	4	0.60	0.10	22.2	5.00	4.43	120
10	—	0.237	0.113	7	1.17	0.23	42.5	10.0	4.25	135
16	—	0.139	0.061	3	0.32	0.09	14.0	2.67	5.25	119
17	1,391	0.223	0.118	3	0.98	0.69	67.5	14.5	4.66	67.8
18	956	0.248	0.152	3	0.88	0.85	114	20.2	5.66	43.6
19	808	0.450	0.256	4	1.52	2.30	150	31.8	4.70	47.8
20	681	0.580	0.360	6	2.45	3.96	237	42.5	5.57	57.6
21	318	0.539	0.336	8	1.90	5.90	235	39.3	5.97	48.3
22	262	0.700	0.474	10	2.35	8.84	317	55.3	5.72	42.5
23	296	0.545	0.336	8	1.75	7.88	252	39.0	6.45	44.9
D-1	—	2.80	2.34	0	4.77	271	3,220	68.3	47.0	69.8
Atm.	—	—	—	—	0.54	—	338	8.17	41.5	65.6

efficient,  $D_b$  (Goldberg and Koide 1962; Guinasso and Schink 1975). It is assumed below that tracer ( $t$ ) distributions (having an activity,  $A$ ) are governed by continuous sedimentation and particle mixing and can be described by:

$$\frac{dA}{dt} = \partial \left( D_b \frac{\partial A}{\partial z} \right) / \partial z - \omega \left( \frac{\partial A}{\partial z} \right) - \lambda A \quad (1)$$

where  $D_b$  (cm<sup>2</sup> yr<sup>-1</sup>) is the biodiffusion coefficient,  $\omega$  (cm yr<sup>-1</sup>) is the sedimentation rate,  $z$  (cm) is the sediment depth, and  $\lambda$  (yr<sup>-1</sup>) is the decay constant for a radioactive tracer. The relatively small depth gradient (<10%) in the sediment solids density permits the assumption that the mixing of porosity is negligible, thereby simplifying the sediment-mixing calculations (Mulsow et al. 1998). At the sediment-water interface ( $z = 0$ ), conservation of mass requires that the flux,  $F(t)$ , of a tracer is balanced by downward transport due to advection and eddy diffusive mixing, respectively, i.e.,

$$F(t) = \omega A - D_b \frac{\partial A}{\partial z}. \quad (2)$$

For tracers having a time-dependent input flux, Eq. 1 and 2 are solved using an implicit finite difference scheme (Boudreau 1986a,b).

For the two-layer model, in which  $D_b$  has a constant value ( $D_b^0$ ) in the SML of depth,  $L$  (cm), and is zero below this depth, Eq. 1 can be solved analytically for tracers, such as <sup>210</sup>Pb, having a constant input flux. The <sup>210</sup>Pb distributions in the mixed layer are given in Christensen (1982), and the <sup>210</sup>Pb activity below the mixed layer (i.e.,  $z \geq L$ ) decreases exponentially with depth,  $z$ :

$$A = A^0 e^{-\beta z} \quad (3)$$

$$\beta = \frac{\lambda}{\omega} \quad (4)$$

where  $\beta$  is the experimentally determined slope of a plot of  $\ln A$  vs. depth,  $z$ , and  $\omega$  is calculated from Eq. 4. However, in most sediment regimes, both the density of organisms and

the energy dissipated in their total burrowing activities tend to decrease with increasing sediment depth. Models employing a depth dependence in  $D_b$  have been developed (Christensen and Bhunia 1986) that are consistent with these physical observations. Mixing in the deeper sediments can be simulated by the model by assigning a constant value to  $D_b$  (expressed as  $D_b^\infty$ ) below the SML. In this case, the general solution of Eq. 1 for a tracer having a constant input flux ( $\partial A / \partial t = 0$ ) permits a linear combination of advective and diffusive transport terms. Under this condition,

$$D_b^\infty(z > L) = \frac{\lambda - \omega\beta}{\beta^2} \quad (5)$$

and all combinations of  $D_b^\infty$  and  $\omega$  satisfying Eq. 5 and the inequality,  $0 < \omega < \lambda/\beta$ , give equivalent <sup>210</sup>Pb profiles (Robbins et al. 1990; Smith et al. 1995).

*Sediment accumulation and mixing rates*—The <sup>210</sup>Pb distributions (Fig. 2) are consistent with the two-layer biodiffusion model outlined above. The change in slope in the excess <sup>210</sup>Pb distributions at the base of the SML was usually sufficiently well defined to permit a visual determination of the mixing depth,  $L$ . The sedimentation rate,  $\omega$  (cm yr<sup>-1</sup>) was estimated from Eq. 3 from a linear least squares correlation between  $\ln A$  and sediment depth,  $z$ , below the mixed layer. Most cores exhibited <sup>210</sup>Pb distributions in the SML consistent with a value for  $D_b^0$  of 10 cm<sup>2</sup> yr<sup>-1</sup>, indicating near-homogeneous mixing, and this was used as the standard value for all of the cores.  $D_b$  was then decreased continuously, using an arctangent function of  $z$ , to a value of 0 at the base of the SML (Boudreau 1986a). The <sup>210</sup>Pb distributions were then simulated by the model (solid lines; Fig. 2) for the values of  $L$  and  $\omega$  given in Table 1. Mass sediment accumulation rates,  $\omega_m$  (g cm<sup>-2</sup> yr<sup>-1</sup>), were also estimated for each core (Table 1) from distributions of <sup>210</sup>Pb activity vs. sediment mass depth (g cm<sup>-2</sup>) below the SML.

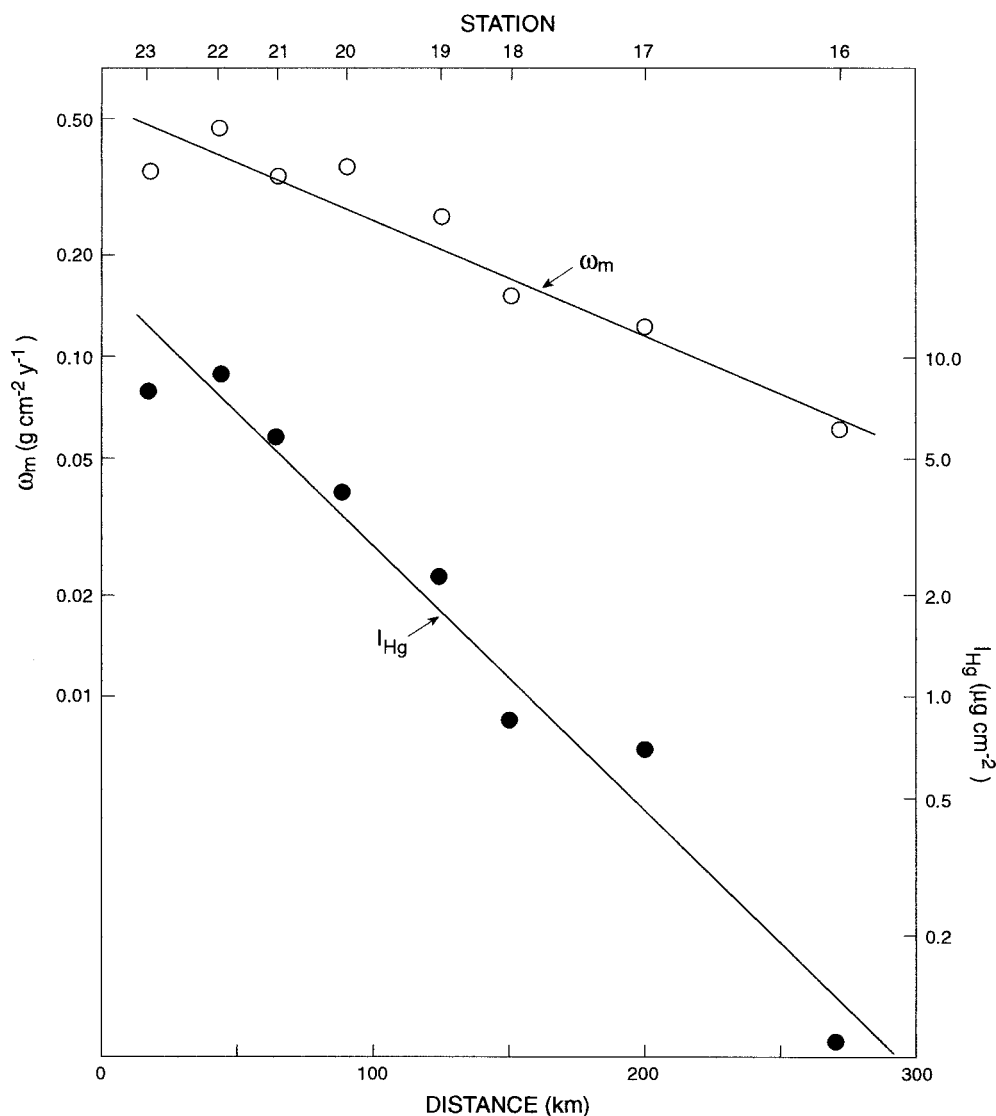


Fig. 3. Sediment accumulation rates,  $\omega_m$  ( $\text{g cm}^{-2} \text{yr}^{-1}$ ), and Hg inventory,  $I_{\text{Hg}}$  ( $\mu\text{g cm}^{-2}$ ), on a semilogarithmic scale vs. station (upper axis) distance (lower axis) seaward from the head of the Laurentian Trough. Solid curves correspond to linear least squares regression of  $\ln \omega_m$  and  $\ln I_{\text{Hg}}$  on distance.

*Sediment mass balance*—Values of  $\omega$  tend to decrease exponentially with increasing distance seaward from Sta. 23 near the head of the Laurentian Trough (Table 1; Fig. 3). This result is consistent with the particle transport model given in Syvitski et al. (1988), in which first-order removal processes are used to characterize the deposition of particles initially held in suspension within the river plume. The sediment inventory deposited each year in the Lower Estuary was estimated using two different methods, as follows.

(1) The depositional area of the Trough ( $5,000 \text{ km}^2$ ) was delineated by the 200-m isobath (Fig. 1) extending from the head of the Trough to Pointe des Monts. The Trough was divided into segments having axial (cross-Trough) boundaries equidistant from adjacent stations (Fig. 1), and each was represented by the station value of  $\omega_m$ . The sum of the products of each segment area and  $\omega_m$  for Sta. 17–23 (Table

1) gave an annual sediment input to the Lower Estuary of  $10.9 \times 10^6 \text{ t yr}^{-1}$ .

(2) Syvitski and Praeg (1989) identified a layer (Unit 5) of Holocene Age, organic-rich muds in the deeper basins of the Trough in a seismic reflection survey. The thickness of this layer (assumed to have been deposited over the last 8,000 yr) decreases from 60 m near the head of the Trough to 10 m at Sta. 17. Values for the Unit 5 thickness divided by 8,000 yr (assuming a sediment mass of  $0.8 \text{ g dry sediment cc wet sediment}^{-1}$ ) are within 30% of the modern sediment accumulation rates,  $\omega_m$  (Table 1), at each station. Integration of Unit 5 thickness under the 200-m isobath in the Lower Estuary gives an annual input of  $8.7 \times 10^6 \text{ t}$ .

The estimate based on Unit 5 sediment thicknesses is less than that based on  $^{210}\text{Pb}$  sediment accumulation rates. However, axial (cross-Trough) gradients in the Unit 5 contours

indicate that sediment deposition is maximized in the central regions of the Trough where the coring stations were located, and therefore, extrapolation of the core results to the entire Laurentian Trough overestimates the total sediment accumulation. This is particularly evident near Sta. 22 at the head of the Trough, where Unit 5 thicknesses decrease from 50 m in the central region to <10 m near the 200-m isobath. If the modern sediment accumulation rates,  $\omega_m$ , from Table 1 are used in conjunction with the axial variations in sediment accumulation delineated by the Unit 5 thicknesses in the Trough sediments, then the annual sediment accumulation rate estimated using Method 1 above is reduced to  $8.8 \times 10^6 \text{ t yr}^{-1}$ . This is greater than estimates in the range of  $6.5 \times 10^6 \text{ t yr}^{-1}$  for the annual sediment input from the St. Lawrence River into the Upper St. Lawrence Estuary (d'Anglejan 1990; Coakley et al. 1993). Additional sources of sediments to the Lower Estuary are clearly required to balance the annual mass budget. These could include biogenic material formed near the head of the Trough, sediments resuspended from sidewall and shallow shelf regions, and material transported in landward flowing bottom waters from the open Gulf (Sundby 1974; Yeats 1988, 1990).

**Mercury results: Saguenay Fjord sediments**—Hg concentration profiles reported for Saguenay Fjord sediments (Barbeau et al. 1981; Smith and Loring 1981; Schafer et al. 1990) indicate that approximately 30 t of mercury presently reside in the fjord, over half (18 t) of which has been retained in sediments in the upper arm of the fjord (Fig. 1). The Hg distribution in core D-1 (Fig. 4) is typical of high sedimentation rate ( $>2 \text{ cm yr}^{-1}$ ) unbioturbated sediments in the upper arm of the fjord, proximal to the mouth of the Saguenay River. The Hg concentration variability in this core is caused by pulsed inputs of sands and silts deposited during periods of high spring river discharge and by inputs from the 1971 St. Jean–Vianney landslide (Smith and Schafer 1987). Core D-1 sediments have been precisely dated (upper axis, Fig. 4) using  $^{210}\text{Pb}$  and fallout radionuclides (Smith et al. 1987). The start-up of the chloralkali plant at Arvida on the Saguenay River in 1947–1948 is reflected in Core D-1 by an increase in Hg above background levels between sediment depths of 100 and 103 cm. A sharp reduction in Hg releases from the chloralkali plant (in response to the imposition of government effluent regulations) between August 1970 and April 1971 is reflected in Core D-1 by an abrupt decline in Hg levels between 42 and 46 cm. Further decreases in Hg levels  $>40 \text{ cm}$  were caused by inputs of Hg-deficient sediment to the fjord from the May 1971 St. Jean–Vianney landslide on the Saguenay River (Smith and Ellis 1982).

**Mercury results: Laurentian Trough sediments**—Hg concentrations in Laurentian Trough cores generally increase from background levels of  $0.03 \mu\text{g g}^{-1}$  measured at depths of  $>60 \text{ cm}$  to a subsurface maximum and then decrease by a factor of approximately 50% toward the sediment–water interface (Fig. 5). The highest levels ( $0.6 \mu\text{g g}^{-1}$ ) were measured in the subsurface maxima of cores at the head of the Trough, whereas levels only marginally above background were measured in cores from the Gulf of St. Lawrence. Hg profiles in Cores 23, 20, 19, and 1 are in agreement with Hg

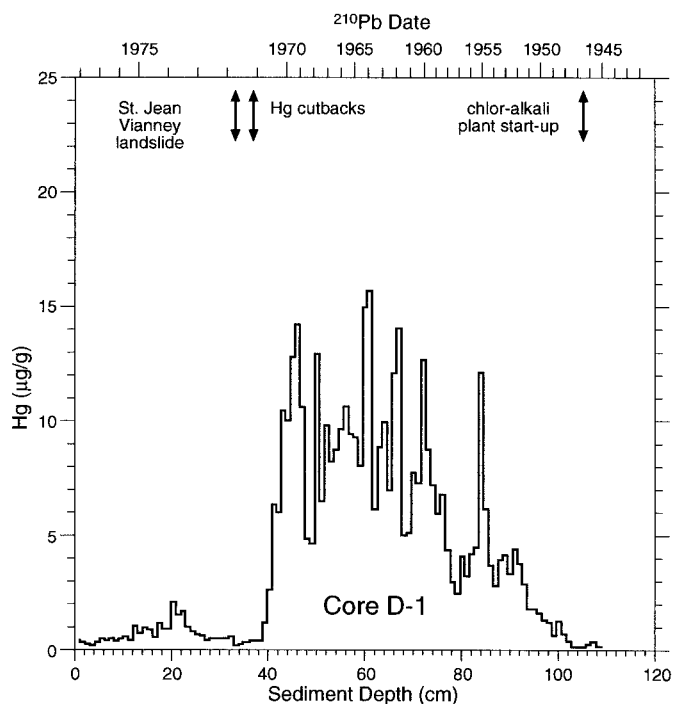


Fig. 4. Hg ( $\mu\text{g g}^{-1}$ ) vs. sediment depth (cm) on bottom axis and vs.  $^{210}\text{Pb}$  date of sediment deposition (upper axis) in the non-bioturbated sediments of Core D-1 from Saguenay Fjord. Increase in Hg above background in 100–103-cm interval is due to chlor-alkali plant start-up in 1947–1948 and decline in 42–46-cm interval is due to decrease in chloralkali plant Hg releases in 1970.

profiles reported by Gobeil and Cossa (1993) for cores independently collected at proximal stations in the Laurentian Trough and Gulf.

The Hg inventories,  $I_{\text{Hg}}$  ( $\mu\text{g cm}^{-2}$ ), in Table 1 have been calculated from Hg and mass-depth ( $\text{g cm}^{-2}$ ) profiles for each core (Fig. 3). Similarly to  $\omega_m$ , the Hg inventory,  $I_{\text{Hg}}$ , decreases exponentially with distance through the Lower Estuary (Fig. 3). However,  $I_{\text{Hg}}$  decreases more rapidly compared to  $\omega_m$ , indicating that the settling of Hg from the river plume is faster than the mean particle settling rate (Syvitski et al. 1988). This may reflect the association of Hg with a more rapidly settling component of the particulate organic load, which is scavenged in the highly productive regions near the head of the Laurentian Trough (Loring 1975).

A total anthropogenic Hg inventory of 130 t for the Lower Estuary was determined from the product of the Hg inventories for each core and sediment areas under the 200-m isobath represented by that core (i.e., Method 1, above). This is within the uncertainties of the Hg inventory estimate of  $170 \pm 85 \text{ t}$  made by Gobeil and Cossa (1993) based on results from three cores in the Lower Estuary. However, regions of reduced modern sediment cover near the head and the sidewalls of the Trough, delineated by the Unit 5 thicknesses (Syvitski and Praeg 1989), probably represent regions of reduced Hg inventories. Using the same factor (0.81) employed above to correct mass sedimentation rates, the estimate of the total Hg inventory for the Lower Estuary becomes 105 t. The Arvida chloralkali plant released at least

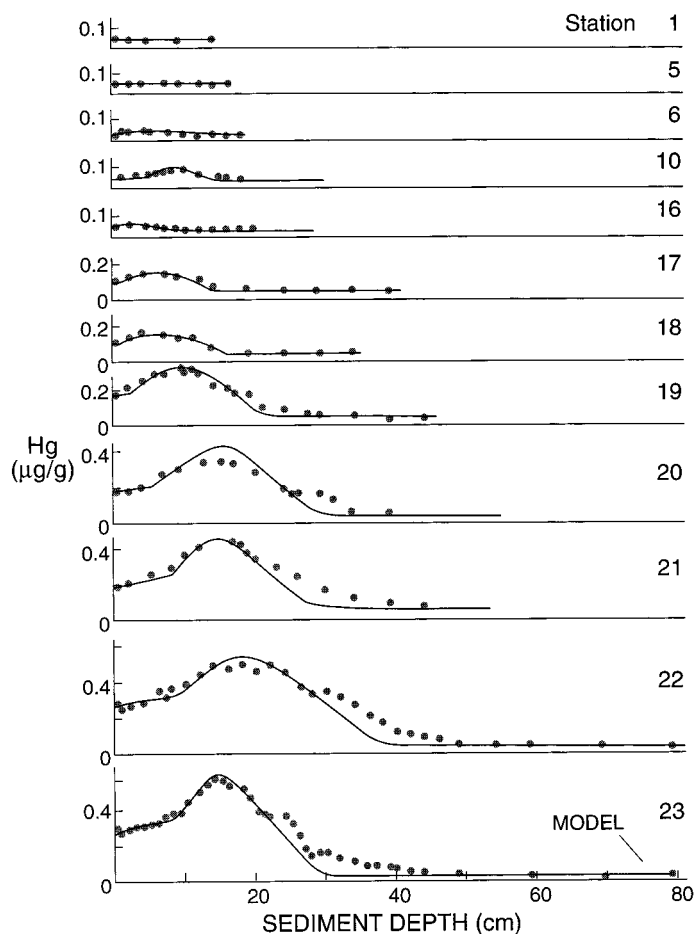


Fig. 5. Hg ( $\mu\text{g g}^{-1}$ ) vs. sediment depth (cm) for bioturbated Laurentian Trough cores. Solid lines represent results of biodiffusion model for values of  $\omega$  and  $L$  given in Table 1 ( $D_b^0 = 10 \text{ cm}^2 \text{ yr}^{-1}$ ,  $D_b^\infty = 0$ ) and Hg input function in Fig. 6.

136 t of Hg, mainly by liquid effluent pathways into the Saguenay River, prior to its eventual closure in 1976 (Loring and Bowers 1978; Ouellet 1979; Smith and Loring 1981). Hence, the Hg inventory of 30 t estimated above for the sediments of the Saguenay Fjord combined with the Hg inventory in the sediments of the St. Lawrence Estuary (100–130 t) approximately balances the minimum quantity (136 t) released by the Arvida chloralkali plant between 1947 and 1976, although an unknown quantity of Hg is still retained within the sediments of the Saguenay River.

**Hg results: Biodiffusion model**—From their measurements of Hg in pore waters in cores from the Lower Estuary, Gobeil and Cossa (1993) estimated that the upward diffusive flux of Hg was 2.6% of the present Hg deposition rate and concluded that the diagenetic remobilization of Hg did not have a significant effect on solid-phase Hg distributions. Hence, Hg sediment profiles probably reflect changes in the input function and can be simulated by the biodiffusion model using model parameters estimated from  $^{210}\text{Pb}$  profiles.

The Hg input function for the St. Lawrence Estuary was assumed to be proportional to Hg effluent releases from the chloralkali plant at Arvida (Fig. 6). This Hg release record

was estimated by Smith and Loring (1981) using the plant's annual record for caustic soda (NaOH) and fluorine production between 1948 and 1971, when the plant sharply curtailed its Hg releases. However, annual inputs of Hg into the Lower Estuary from the St. Lawrence River may still have been as great as 0.5 t/yr in dissolved phases and 2.0 t/yr in particulate phases well into the 1980s (Cossa et al. 1988; Cossa 1990). The post-1971 extension of the Hg input function was estimated from a time series of Hg concentrations measured in shrimp tissue collected in the Saguenay Fjord during the 1970s and 1980s (Cossa 1990). Relative values for the Hg input function to the St. Lawrence Estuary were estimated by normalization of the two separate input functions (accounting for their different units) at their 1970 values. The Hg input function in Fig. 6 was then introduced into the biodiffusion model to simulate Hg sediment profiles (solid lines, Fig. 5), using model parameter values for each core derived from the  $^{210}\text{Pb}$  results (Table 1). Hg concentrations predicted by the model were normalized to the measured values at the sediment–water interface.

Notable features of the model results are that they accurately simulate both the Hg concentration gradients through the SML and the position and magnitude of the subsurface maxima in most cores. One discrepancy is that Hg threshold horizons are predicted at shallower depths than those measured in the cores (e.g., Figs. 6, 7). One possible explanation is that Hg inputs to the Lower Estuary from the St. Lawrence River preceded the 1947 construction of the chloralkali plant on the Saguenay River. Hg contamination of sediments  $>6 \mu\text{g g}^{-1}$  has been measured in Lac St. Francois and Lac St. Louis, both proximal to chloralkali plants on the St. Lawrence River (Jarry et al. 1985). The Hg distributions indicate that the sources of Hg contamination are local sources within the river or estuary and are not derived from Lake Ontario (Allan 1988, 1990), which is, itself, an efficient particle trap. Hg levels  $>1 \mu\text{g g}^{-1}$ , measured in a core collected in the upper St. Lawrence Estuary (Coakley et al. 1993), are more difficult to interpret because the sediment regime appears to be one of active mixing or particle resuspension. However, significant downstream transport of Hg from chloralkali plants at locations such as Shawanigan, which began operations in 1939, cannot be discounted until Hg profiles have been more accurately dated in upstream basins of the St. Lawrence River.

A second explanation for the occurrence of Hg horizons below those predicted by the model is that mixing is not solely confined to the SML but extends deeper in the sediments. Deeper mixing can be accommodated in the biodiffusion model by assigning a nonzero value to the biodiffusion coefficient,  $D_b^\infty$ , for the bottom sediment layer ( $z \geq L$ ). As noted above, linear combinations of  $\omega$  and  $D_b^\infty$  satisfying Eq. 5 give approximately equivalent  $^{210}\text{Pb}$  profiles below the SML, with the effect of increased mixing balanced by a slightly reduced sedimentation rate. Hence, the model was run for Core 23 using values for  $D_b^0$ ,  $D_b^\infty$ , and  $\omega$  given in Fig. 7, with  $D_b(z)$  being decreased as a function of sediment depth, from  $D_b^0$  in the SML to a constant value,  $D_b^\infty$  ( $z \geq L$ ). The actual zone of deep mixing was limited to 50 cm. These parameter values have little effect on the  $^{210}\text{Pb}$  profile, but mixing below the SML results in the deeper extension of

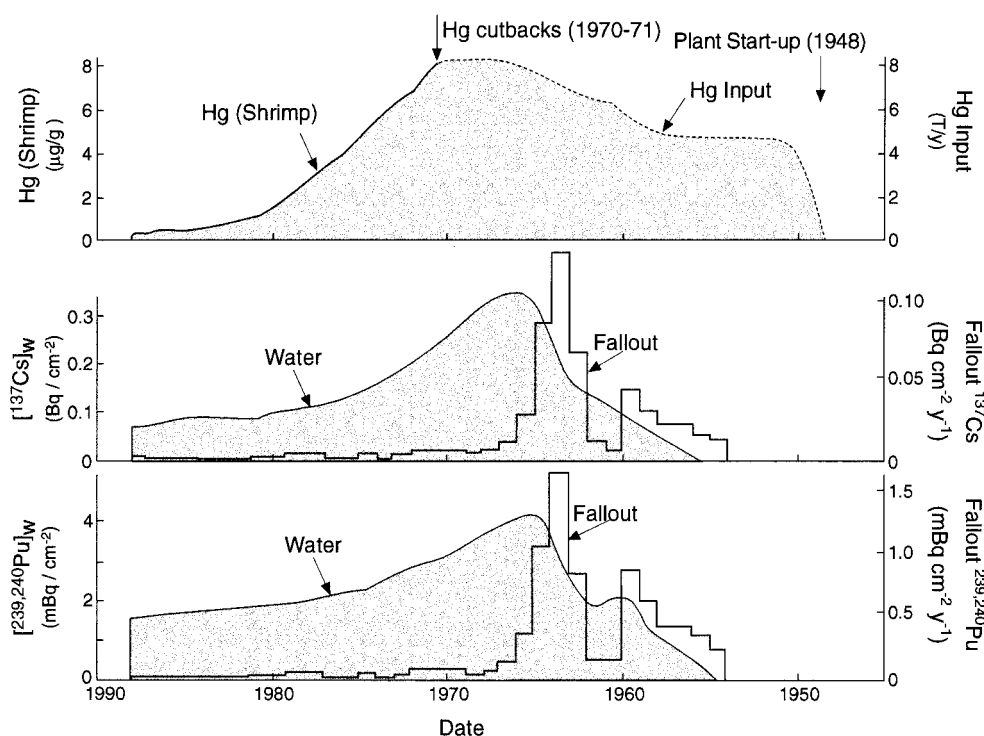


Fig. 6. Upper panel: Hg input function for biodiffusion model used to simulate Hg sediment profiles in Lower St. Lawrence Estuary estimated (1947–1971) from Hg releases (t/yr) from Arvida chloralkali plant (Smith and Loring 1981) and during 1971–1987 from Hg concentrations in shrimp tissue from Saguenay Fjord (Cossa 1990). Lower panels:  $^{137}\text{Cs}$  and  $^{239,240}\text{Pu}$  (solid lines) water column inventories estimated from St. Lawrence drainage basin model ( $T_{DB} = 1,000$  and  $3,000$  yr, respectively,  $T_w = 5$  yr) used as input functions in biodiffusion model to simulate Laurentian Trough core profiles. Dotted lines represent atmospheric fallout input functions for  $^{137}\text{Cs}$  and  $^{239,240}\text{Pu}$ .

the Hg threshold horizon. Better agreement between experimental and model Hg profiles was found for all other St. Lawrence Estuary cores when limited mixing was permitted below the SML.

*$^{137}\text{Cs}$  and  $^{239,240}\text{Pu}$ : Drainage basin model*— $^{137}\text{Cs}$  and  $^{239,240}\text{Pu}$  are particle-reactive fallout radionuclides whose transport into the Estuary and Gulf of St. Lawrence occurs both from direct atmospheric inputs and by advective transport both from the Atlantic Ocean and from the St. Lawrence River drainage basin. However, the elevated particle reactivity of  $^{137}\text{Cs}$  and  $^{239,240}\text{Pu}$  (Hamilton-Taylor et al. 1993) in freshwater compared to marine systems suggests that the primary transport mechanism is by adsorption onto particles in the St. Lawrence drainage basin and subsequent transport through the St. Lawrence River. The drainage basin of the Gulf of St. Lawrence has a total area of  $1,500,000 \text{ km}^2$ , part of which ( $770,000 \text{ km}^2$ ) consists of the urbanized and cultivated Great Lakes drainage basin; the other part, which includes the Ottawa River ( $146,000 \text{ km}^2$ ) and Saguenay River ( $78,000 \text{ km}^2$ ) watersheds, is typified by the forested, more sparsely settled landscape of the Canadian Shield. The flux of particle-reactive fallout radionuclides through the Great Lakes system has been calculated by Robbins (1985a,b) using a model that includes the effects of soil erosion from the drainage basin, particle settling, resuspension, and other first-

order biogeochemical processes. The model results for the time-dependent water column concentrations of  $^{137}\text{Cs}$  and  $^{239,240}\text{Pu}$  in Lake Ontario between 1950 and 1990 can be used to estimate the source terms for the transport of these radionuclides from the outlet of Lake Ontario into the St. Lawrence River at Cornwall, Ontario (Robbins 1985b).

A reconstruction of the history of fallout radionuclide transport through the St. Lawrence River can be estimated using a drainage basin model (Smith and Ellis 1982; Smith et al. 1987) previously applied to the Saguenay River watershed. The St. Lawrence River drainage basin, downstream from Lake Ontario, is separated into two components: (1) a water column component (also referred to as the rapid transport component by Dominik et al. [1987] and Joshi and Shukla [1991]), which includes the St. Lawrence River, its tributaries, and catchment basins having a total surface area,  $S_w$ , of approximately  $7,300 \text{ km}^2$ , and (2) a terrestrial (soil) component having a surface area,  $S_{DB}$ , of  $730,000 \text{ km}^2$ . The time-dependent atmospheric flux of fallout radionuclides to both components of the drainage basin can be approximated by that for  $^{90}\text{Sr}$  for New York City (Monetti and Larsen 1991), multiplied by a factor of 1.5 for  $^{137}\text{Cs}$  (1952–1987) and factors of 0.012 (1952–1960) and 0.018 (1960–1987) for  $^{239,240}\text{Pu}$  (Fig. 6), representative of the relative fallout fluxes (Robbins 1985a; Smith et al. 1987). The time-dependent inventories ( $\text{Bq cm}^{-2}$ ) of radionuclides in the soil,  $[A]_{\text{soil}}$

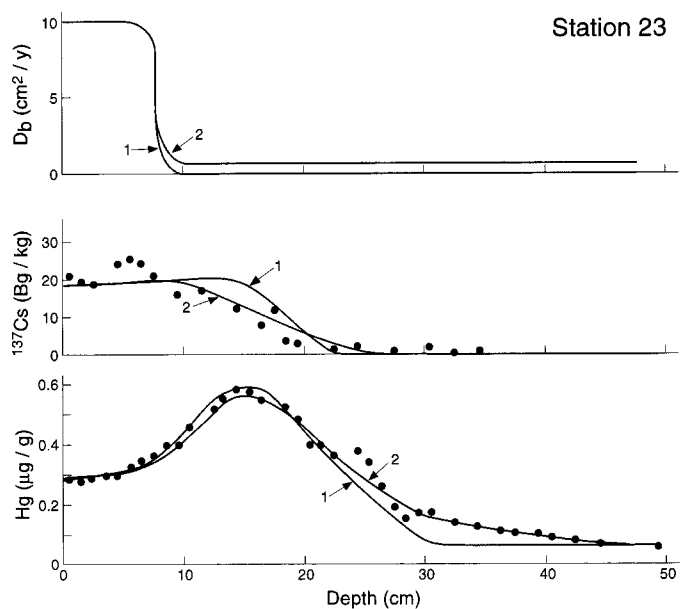


Fig. 7. The effect of sediment mixing below the SML ( $L = 8$  cm) is illustrated for Hg and  $^{137}\text{Cs}$  profiles in Core 23. Upper Panel: Variation of  $D_b$  with sediment depth from  $D_b^0 = 10 \text{ cm}^2 \text{ yr}^{-1}$  to  $D_b^\infty = 0$  (Case 1) and  $D_b^\infty = 0.5 \text{ cm}^2 \text{ yr}^{-1}$  (Case 2). Lower Panels: Model  $^{137}\text{Cs}$  and Hg profiles for Case 1 ( $D_b^0 = 0$ ,  $\omega = 0.545 \text{ cm yr}^{-1}$ ) and Case 2 ( $D_b^0 = 0.50 \text{ cm}^2 \text{ yr}^{-1}$ ;  $\omega = 0.516 \text{ cm yr}^{-1}$ ) are compared to sediment profiles.

and water column,  $[A]_w$  are governed by first-order differential equations that can be numerically integrated for given values of the radionuclide residence times in the water column,  $T_w$ , and soils of the drainage basin,  $T_{DB}$ , respectively. The critical assumption in this model is that radionuclide transport from the soil to the water components of the drainage basin occurs by leaching and particle transport associated with the erosion of soils and can be characterized by a first-order rate constant proportional to  $1/T_{DB}$ .

$^{137}\text{Cs}$  and  $^{239,240}\text{Pu}$  residence times ( $T_{DB}$ ) of 1,000 and 3,000 yr, respectively, previously estimated (Smith et al. 1987) for the soil component of the Saguenay River drainage basin, should be equally applicable to the St. Lawrence River drainage basin. However, the radionuclide water column residence time,  $T_w$ , of 1 yr for the Saguenay River system probably represents a lower limit on the residence time for transport through the much larger river network of the St. Lawrence River watershed. The water residence time in the St. Lawrence River from Lake Ontario to the Gulf of St. Lawrence is  $<1$  yr, but catchment basins along the St. Lawrence River, including three riverine lakes, cause additional delays in particle transport and can increase the radionuclide residence time in the aquatic water column. Mass-balance studies of mirex transport between Lake Ontario and the sediments of the Lower Estuary (Comba et al. 1993) indicate that transport of particle-reactive contaminants between these two systems may take 3–5 yr. Based on these considerations, a mean residence time of  $T_w = 5$  yr has been used to estimate  $^{137}\text{Cs}$  and  $^{239,240}\text{Pu}$  transport through the water column component of the St. Lawrence River drainage basin model.

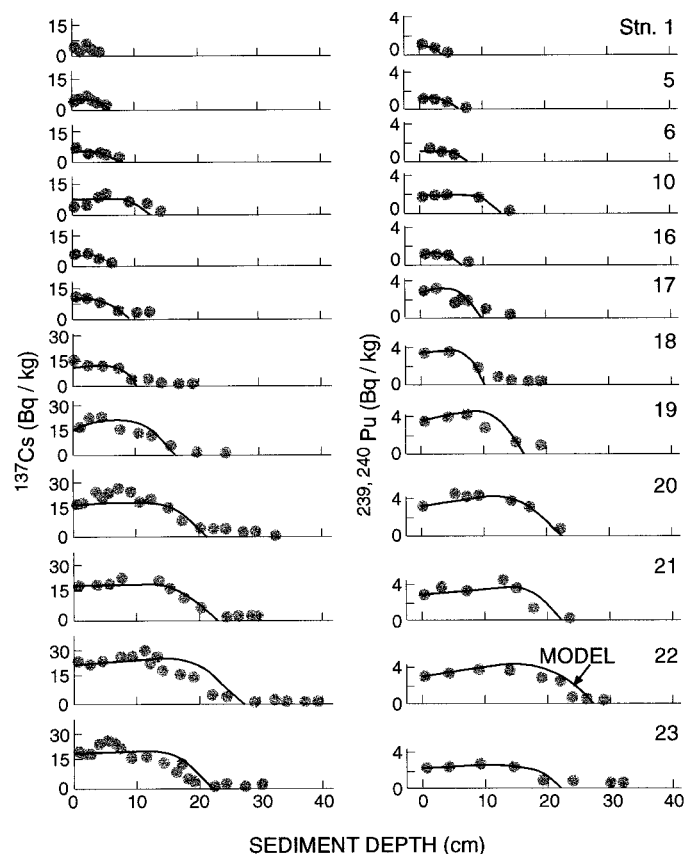


Fig. 8. Data points represent  $^{137}\text{Cs}$  and  $^{239,240}\text{Pu}$  results ( $\text{Bq kg}^{-1}$ ) for Laurentian Trough cores. Solid lines are the results of biodiffusion model for values of  $\omega$  and  $L$  given in Table 1 ( $D_b^0 = 10 \text{ cm}^2 \text{ yr}^{-1}$ ,  $D_b^\infty = 0$ ) and sediment input functions illustrated in Fig. 6, calculated using the St. Lawrence drainage basin model.

*$^{137}\text{Cs}$  and  $^{239,240}\text{Pu}$ : Biodiffusion model*—The time-dependent radionuclide inventories in the water column,  $[A]_w$ , calculated from the drainage basin model, are illustrated in Fig. 6 for  $^{137}\text{Cs}$  (using values of  $T_{DB} = 1,000$  yr;  $T_w = 5$  yr) and  $^{239,240}\text{Pu}$  ( $T_{DB} = 3,000$  yr;  $T_w = 5$  yr).  $^{137}\text{Cs}$  and  $^{239,240}\text{Pu}$  inputs from Lake Ontario outflow based on Robbin's (1985a,b) results contribute  $<5\%$  to the inventories estimated above, reflecting the efficiency of Lake Ontario as a particle trap, and have been neglected in the present case. Using these water column inventories as input functions for the biodiffusion model and normalizing model results to radionuclide activities at the sediment–water interface, sediment  $^{137}\text{Cs}$  and  $^{239,240}\text{Pu}$  profiles have been calculated using the values of  $\omega$  and  $L$  given in Table 1 ( $D_b^0 = 10 \text{ cm}^2 \text{ yr}^{-1}$ ;  $D_b^\infty = 0$ ). Good agreement between model and experimental results (Fig. 8) is obtained for both  $^{137}\text{Cs}$  and  $^{239,240}\text{Pu}$  using  $T_w = 5$  yr. However, as in the case of the Hg distributions, the model predicts depths for the appearance of  $^{137}\text{Cs}$  and  $^{239,240}\text{Pu}$  threshold horizons shallower than those actually observed (Fig. 8). Since there is little uncertainty regarding the initial appearance of fallout radionuclides in the environment, the most likely cause of this discrepancy is sediment mixing below the SML. The same values of  $\omega$  and used to simulate deep mixing of Hg below the SML also provide better agreement

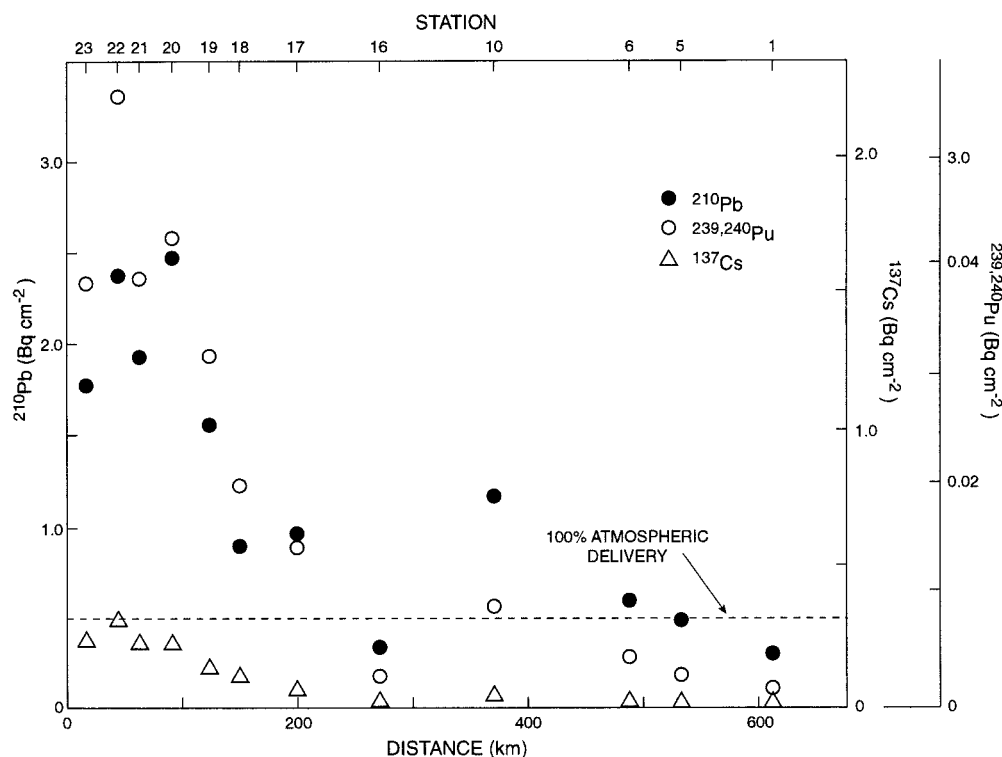


Fig. 9.  $^{210}\text{Pb}$ ,  $^{239,240}\text{Pu}$ , and  $^{137}\text{Cs}$  sediment inventories ( $\text{Bq cm}^{-2}$ ) plotted as a function of distance seaward through the St. Lawrence Estuary and Gulf from the head of the Laurentian Trough. Station numbers are given on upper axis. Dotted line corresponds to the cumulative inventories for 100% efficient retention of atmospheric inputs.

between model and experimental  $^{137}\text{Cs}$  profiles for Core 23 (Fig. 7).

**Radionuclide inventories**— $^{137}\text{Cs}$ ,  $^{239,240}\text{Pu}$ , and  $^{210}\text{Pb}$  inventories for St. Lawrence Estuary and Gulf cores (Fig. 9) are compared in Table 1 with results from Core D-1 from the Saguenay Fjord (Fig. 1) and cumulative (for  $^{210}\text{Pb}$ , steady-state) atmospheric inputs.  $^{210}\text{Pb}$  and  $^{239,240}\text{Pu}$  inventories in the Saguenay Fjord (D-1) and Lower Estuary (Sta. 17–23) sediments are greater than those predicted by 100% efficient retention of the atmospheric flux (indicated by dotted line in Fig. 9), due to high sedimentation rates and the focusing of direct fallout and erosional inputs from the drainage basin. Although  $^{137}\text{Cs}$  inventories are high in the Saguenay Fjord, where the sediments reflect the particle load transported directly from the Saguenay River, they are substantially reduced in Lower Estuary sediments, mainly because of desorption of  $^{137}\text{Cs}$  from riverborne particles during transport through the higher salinity waters of the St. Lawrence Estuary.

The radionuclide inventories and areas representative of each station given in Table 1 have been used to estimate the total radionuclide inventories for the sediments of the Lower Estuary, and these values are compared to predicted inputs from the St. Lawrence River in Table 2. The  $^{239,240}\text{Pu}$  sediment inventory in the Lower Estuary estimated using the areal contours given in Table 1 is 1.37 TBq. This reduces to a value of 1.10 TBq if axial changes in sedimentation rate

based on Unit 5 thicknesses (Syvitski and Praeg 1989) are considered. For a  $^{239,240}\text{Pu}$  drainage basin residence time of 3,000 yr, the annual erosional removal of  $^{239,240}\text{Pu}$  is 0.023% each year or approximately 0.58% of the cumulative  $^{239,240}\text{Pu}$  fallout inventory ( $8.17 \text{ mBq cm}^{-2}$ ; Table 1) in 25 yr. For a drainage basin of  $730,000 \text{ km}^2$ , this corresponds to the total erosional transport of 0.35 TBq of  $^{239,240}\text{Pu}$  into the water column (river). The fallout input into the water column from direct atmospheric deposition (equal to the product of the water column area [ $7,300 \text{ km}^2$ ] and the cumulative fallout  $^{239,240}\text{Pu}$  inventory [ $8.17 \text{ mBq cm}^{-2}$ ]) is 0.60 TBq. The sum of the erosional and direct fallout  $^{239,240}\text{Pu}$  inputs into the water column is 0.95 TBq of  $^{239,240}\text{Pu}$ , which approximately balances the 1.10 TBq measured in Lower Estuary sediments (Table 2). This result indicates that the drainage basin model provides a reasonable estimate of  $^{239,240}\text{Pu}$  transport through the St. Lawrence River watershed and that virtually all of the riverborne  $^{239,240}\text{Pu}$  is deposited in the sediments of the Lower Estuary. A similar calculation for  $^{137}\text{Cs}$  ( $T_{DB} = 1,000 \text{ yr}$ ) gives a total input from the St. Lawrence River of 68 TBq. The river input is one order of magnitude greater than the  $^{137}\text{Cs}$  inventory of 6 TBq (Table 2) calculated for the sediments of the Lower Estuary. This result is consistent with observations above that most of the riverborne  $^{137}\text{Cs}$  undergoes desorption from particles as they enter the high ionic strength seawater of the Lower Estuary.

The steady-state removal flux,  $F_w^{\text{Pb-210}}$  ( $\text{Bq yr}^{-1}$ ) of  $^{210}\text{Pb}$  from the water column (river) component of the St.

Table 2. Steady-state inputs of suspended particulate matter and  $^{210}\text{Pb}$  from the St. Lawrence River and cumulative inputs of the transient contaminants Hg,  $^{239,240}\text{Pu}$ , and  $^{137}\text{Cs}$  are compared to the fluxes and inventories measured in the sediments of the Lower St. Lawrence Estuary. Sediment inventories and fluxes have been calculated from data in Table 1, decreased by a correction factor of 0.81 intended to compensate for axial (cross-channel) gradients (thinning) in sediment thickness. The radionuclide inputs from the river were estimated from a drainage basin model as outlined in the text.

Steady-state inputs	Steady-state river input	Sediment flux	Transient inputs	Cumulative river input	Sediment inventory
SPM	$6.5 \times 10^6$ t/yr*	$8.7 \times 10^6$ t/yr	Hg	136 t‡	105
$^{210}\text{Pb}$	1.7 TBq/yr†	1.7 TBq/yr	$^{239,240}\text{Pu}$	0.95 TBq†	1.1 TBq
			$^{137}\text{Cs}$	68 TBq†	6 TBq

\* Coakley et al. (1993).

† Calculated from the drainage basin model (Smith et al. 1987).

‡ Smith and Loring (1981).

Lawrence River drainage basin is given analytically by the drainage basin model ( $T_{DB} = 3,000$  yr;  $T_w = 5$  yr; Smith et al. 1987):

$$F_w^{\text{Pb-210}} = \left( \frac{1}{1 + \frac{T_w}{T_{1/2}}} \right) F_{\text{atm}}^{\text{Pb-210}} \left( S_w + S_{DB} \left[ \frac{1}{1 + \frac{T_{DB}}{T_{1/2}}} \right] \right) \quad (6)$$

where  $F_{\text{atm}}^{\text{Pb-210}}$  is the atmospheric flux ( $0.017$  Bq  $\text{cm}^{-2}$   $\text{yr}^{-1}$ ) and  $T_{1/2}$  is the  $^{210}\text{Pb}$  half-life (22.3 yr). The first term in brackets on the right-hand side of Eq. 6 represents the fractional radioactive decay undergone by  $^{210}\text{Pb}$  during its transport through the water column, and the remaining part of the expression represents the steady-state input to the water column from direct fallout and erosional transport from the drainage basin. The  $^{210}\text{Pb}$  removal flux from the river given by Eq. 6 is  $1.7$  TBq  $\text{yr}^{-1}$ . This is accurately balanced by the steady-state  $^{210}\text{Pb}$  inventory measured in Lower Estuary sediments of  $55$  TBq, corresponding to a steady-state flux ( $^{210}\text{Pb}$  inventory  $\times \ln 2/T_{1/2}$ ) of  $1.7$  TBq  $\text{yr}^{-1}$  (Tables 1, 2).

The  $^{137}\text{Cs}/^{239,240}\text{Pu}$  and  $^{210}\text{Pb}/^{239,240}\text{Pu}$  inventory ratios in Core D-1 (Table 1) are similar to those predicted from fallout, owing to the limited fractionation that occurs among these radionuclides in small watersheds. However, the mean  $^{210}\text{Pb}/^{239,240}\text{Pu}$  inventory ratio of 50 for cores (Sta. 17–23) in the St. Lawrence Estuary is significantly smaller than the ratio of 70 measured in Core D-1 in the Saguenay Fjord (Table 1). This decrease can be partially accounted for by radioactive decay of  $^{210}\text{Pb}$  during its longer residence time ( $T_w = 5$  yr) in the larger watershed of the St. Lawrence River compared to that ( $T_w = 1$  yr) in the Saguenay River. This is illustrated analytically by the term,  $1/(1 + T_w/T_{1/2})$  in Eq. 6, which indicates that the  $^{210}\text{Pb}$  inventory will decay by an additional 15% during transit through a watershed having  $T_w = 5$  yr compared to a watershed having  $T_w = 1$  yr (other parameters remaining constant), a decrease that partly accounts for the decreased  $^{210}\text{Pb}/^{239,240}\text{Pu}$  inventory ratios in the St. Lawrence Estuary compared to the head of the Saguenay Fjord. In contrast, the  $^{210}\text{Pb}/^{239,240}\text{Pu}$  inventory ratio increases by a factor of two between the Lower Estuary (Sta. 17–22) and the Gulf of St. Lawrence (Sta. 1–16) sediments (Table 1). This reflects the reduced importance of riverine compared

to direct atmospheric inputs of  $^{210}\text{Pb}$  and fallout radionuclides to the Gulf. The greater  $^{210}\text{Pb}/^{239,240}\text{Pu}$  inventory ratios in Gulf sediments result from the greater scavenging efficiency for the removal of  $^{210}\text{Pb}$ , compared to  $^{239,240}\text{Pu}$ , from dissolved seawater phases onto particles and the fact that much of the fallout  $^{239,240}\text{Pu}$  inventory from the 1960s is still retained in the water column. Further, in situ production of  $^{210}\text{Pb}$  from dissolved  $^{226}\text{Ra}$  in seawater provides an additional source of  $^{210}\text{Pb}$ , which may influence these relative inventories. Buesseler et al. (1986) also observed a decrease in the  $^{210}\text{Pb}/^{239,240}\text{Pu}$  inventory ratio, with increasing water depth in shelf and slope sediments off the northeast U.S.A.

## Conclusions

Sediment accumulation rates, determined from the application of a two-layer biodiffusion model to  $^{210}\text{Pb}$  profiles measured in sediment cores collected along the Laurentian Trough, decrease from  $0.70$   $\text{cm yr}^{-1}$  ( $0.47$   $\text{g cm}^{-2}$   $\text{yr}^{-1}$ ) near the head of the Trough in the Lower Estuary to  $0.04$   $\text{cm yr}^{-1}$  ( $0.03$   $\text{g cm}^{-2}$   $\text{yr}^{-1}$ ) in the Gulf of St. Lawrence. The sediment load deposited in the Lower Estuary each year estimated from the product of the measured sediment accumulation rates and areas under the 200-m isobaths is  $8.8 \times 10^6$  t/yr when axial (cross-channel) gradients in sediment accumulation are estimated from seismic reflection data. Additional sediment sources are required to balance the  $6.5 \times 10^6$  t/yr of material transported through the St. Lawrence River system.

Hg profiles in Lower St. Lawrence sediments were simulated using a two-layer biodiffusion model with model parameters determined from  $^{210}\text{Pb}$  distributions and an Hg input function based on the historical record (1947–1976) of releases from a chloralkali plant located on the Saguenay River. The Hg inventory estimated for the Lower Estuary of 105–130 t added to the 30 t of Hg buried in the sediments of the Saguenay Fjord approximately balances the 136 t of Hg released by the Arvida chloralkali plant. Fallout radionuclide ( $^{137}\text{Cs}$ ,  $^{239,240}\text{Pu}$ ) profiles were simulated with the biodiffusion model using input functions estimated from a drainage basin model that invokes residence times in the St. Lawrence drainage basin of 1,000 and 3,000 yr for  $^{137}\text{Cs}$  and

<sup>239,240</sup>Pu, respectively, and a water column residence time of 5 yr. Agreement between model and experimental results is improved when mixing is permitted to extend below the SML. <sup>210</sup>Pb and <sup>239,240</sup>Pu inventories in the sediments from the Lower Estuary are balanced by river fluxes predicted by the drainage basin model, while <sup>137</sup>Cs sediment inventories are much lower because of <sup>137</sup>Cs desorption from particles during transit through the estuary.

## References

- ALLAN, R. J. 1988. Toxic chemical pollution of the St. Lawrence River (Canada) and its Upper Estuary. *Water Sci. Technol.* **20**: 77–88.
- . 1990. The Saguenay Fjord: A third factor in the toxic chemical contamination of the St. Lawrence Estuary. *Water Pollut. Res. J. Can.* **25**: 1–14.
- BARBEAU, C., R. BOUGIÉ, AND J. E. COTÉ. 1981. Temporal and spatial variations of mercury, lead, zinc and copper in sediments of the Saguenay Fjord. *Can. J. Earth Sci.* **18**: 1065–1074.
- BOUDREAU, B. P. 1986a. Mathematics of tracer mixing in sediments: I. Spatially-dependent, diffusive mixing. *Am. J. Sci.* **286**: 161–198.
- . 1986b. Mathematics of tracer mixing in sediments: II. Non-local mixing and biological conveyor-belt phenomena. *Am. J. Sci.* **286**: 199–238.
- BUESSELER, K., H. L. LIVINGSTON, AND E. R. SHOLKOVITZ. 1986. <sup>239,240</sup>Pu and excess <sup>210</sup>Pb inventories along the shelf and slope of the northeast U.S.A. *Earth Planet. Sci. Lett.* **76**: 10–22.
- CARPENTER, R., M. L. PETERSON, AND J. T. BENNETT. 1982. <sup>210</sup>Pb-derived sediment accumulation and mixing rates for the Washington continental slope. *Mar. Geol.* **48**: 1152–1172.
- CHRISTENSEN, E. R. 1982. A model for radionuclides in sediments influenced by mixing and compaction. *J. Geophys. Res.* **87**: 566–572.
- , AND P. K. BHUNIA. 1986. Modelling radiotracers in sediments: Comparison with observations in Lakes Huron and Michigan. *J. Geophys. Res.* **91**: 8559–8571.
- COAKLEY, J. P., E. NAGY, AND J-B. SERODES. 1993. Spatial and vertical trends in sediment-phase contaminants in the upper estuary of the St. Lawrence River. *Estuaries* **16**: 653–669.
- COMBA, M. E., R. J. NORSTROM, C. R. MACDONALD, AND K. L. E. KAISER. 1993. A Lake Ontario–Gulf of St. Lawrence dynamic mass balance for mirex. *Environ. Sci. Technol.* **27**: 2198–2206.
- COSSA, D. 1990. Chemical contaminants in the St. Lawrence Estuary and Saguenay Fjord. *Coastal and estuarine studies*, 39, p. 239–268. *In* M. El-Sabh and N. Silverberg [eds.], *Oceanography of a large scale estuarine system, the St. Lawrence*. Springer-Verlag.
- , C. GOBEIL, AND P. COURAU. 1988. Dissolved mercury behaviour in the Saint Lawrence Estuary. *Estuarine Coastal Shelf Sci.* **26**: 227–230.
- D'ANGLEJAN, B. 1990. Recent sediments and sediment transport processes in the St. Lawrence Estuary. *Coastal and estuarine studies*, 39, p. 109–129. *In* M. El-Sabh and N. Silverberg [eds.], *Oceanography of a large scale estuarine system, the St. Lawrence*. Springer-Verlag.
- DOMINIK, J., D. BURRUS, AND J-P. VERNET. 1987. Transport of the environmental radionuclides in an alpine watershed. *Earth Planet. Sci. Lett.* **84**: 165–180.
- GAGNE, J. A., AND M. SINCLAIR. 1991. Marine fisheries resources and oceanography of the St. Lawrence Estuary. *Coastal and Estuarine Studies*, 39, p. 358–377. *In* M. El-Sabh and N. Silverberg [eds.], *Oceanography of a large scale estuarine system, the St. Lawrence*. Springer-Verlag.
- GAGNON, C., E. PELLETIER, A. MUCCI, AND W. FITZGERALD. 1996. Diagenetic behavior of methylmercury in organic-rich coastal sediments. *Limnol. Oceanogr.* **41**: 428–434.
- GOBEIL, C., AND D. COSSA. 1993. Mercury in sediments and sediment pore water in the Laurentian Trough. *Can. J. Fish. Aquat. Sci.* **50**: 1794–1800.
- GOLDBERG, E., AND M. KOIDE. 1962. Geochronological studies of deep sea sediments by the ionium/thorium method. *Geochim. Cosmochim. Acta* **26**: 417–450.
- GUINASSO, N., AND D. SCHINK. 1975. Quantitative estimates of biological mixing rates in abyssal sediments. *J. Geophys. Res.* **80**: 3032–3043.
- HAMILTON-TAYLOR, J., M. KELLY, J. G. TITLEY, AND D. R. TURNER. 1993. Particle-solution behaviour of plutonium in an estuarine environment, Esk Estuary, UK. *Geochim. Cosmochim. Acta* **57**: 3367–3381.
- JARRY, V., P. ROSS, L. CHAMPOUX, H. SLOTERDIJK, A. MURDOCH, Y. COUILLARD, AND F. LAVOIE. 1985. Repartition spatiale des contaminants dans les sédiments du Lac St.-Louis (Fleuve St.-Laurent). *Water Pollut. Res. J. Can.* **20**: 75–99.
- JOSHI, S. R., AND B. S. SHUKLA. 1991. The role of the water/soil distribution coefficient in the watershed transport of environmental radionuclides. *Earth Planet. Sci. Lett.* **105**: 314–318.
- LORING, D. H. 1975. Mercury in the sediments of the Gulf of St. Lawrence. *Can. J. Earth Sci.* **12**: 1219–1237.
- . 1988. Trace metal geochemistry of Gulf of St. Lawrence sediments. *In* P. M. Strain [ed.], *Chemical oceanography in the Gulf of St. Lawrence*. *Can. Bull. Fish. Aquat. Sci.* **220**: 99–122.
- , AND J. M. BEWERS. 1978. Geochemical mass balances for mercury in a Canadian fjord. *Chem. Geol.* **22**: 309–330.
- , AND D. J. G. NOTA. 1973. Morphology and sediments of the Gulf of St. Lawrence. *Bull. Fish. Res. Board Can.* **182**: 1–147.
- , AND R. T. T. RANTALA. 1992. Manual for the geochemical analyses of marine sediments and suspended particulate matter. *Earth-Sci. Rev.* **32**: 235–283.
- MASSE, R., D. MARTINEAU, L. TREMBLAY, AND P. BELAND. 1986. Concentrations and chromatographic profile of DDT metabolites and polychlorobiphenyl (PCB) residues in stranded beluga whales (*Delphinapterus leucas*) from the St. Lawrence Estuary. *Arch. Environ. Contam. Toxicol.* **15**: 567–579.
- MONETTI, M. A., AND R. J. LARSEN. 1991. Worldwide deposition of strontium-90 through 1986. *Environmental Measurements Laboratory*. EML-533.
- MULSOW, S., B. P. BOUDREAU, AND J. N. SMITH. 1998. Bioturbation and porosity gradients. *Limnol. Oceanogr.* **43**: 1–9.
- OLSEN, C. R., H. J. SIMPSON, T-H. PENG, R. F. BOOP, AND R. M. TRIER. 1981. Sediment mixing and accumulation rate effects on radionuclide depth profiles in Hudson Estuary sediments. *J. Geophys. Res.* **86**: C11, 11020–11028.
- OUELLET, M. 1979. Géochemie et granulométrie des sédiments superficiels du Lac Saint-Jean et de la rivière Saguenay. *INRS-EAU, Rapport scientifique*, 104.
- ROBBINS, J. A. 1985a. Great lakes regional fallout source functions. *Great Lakes Environmental Research Laboratory Tech. Memo. ERL-GLERL-56*.
- . 1985b. The coupled lakes model for estimating the long-term response of the Great Lakes to time-dependent loadings of particle associated contaminants. *Great Lakes Environmental Research Laboratory Tech. Memo. ERL-GLERL-57*.
- , AND D. N. EDGINGTON. 1975. Determination of recent sedimentation rates in Lake Michigan using <sup>210</sup>Pb and <sup>137</sup>Cs. *Geochim. Cosmochim. Acta* **39**: 285–304.

- , A. MUDROCH, AND B. G. OLIVER. 1990. Transport and storage of  $^{137}\text{Cs}$  and  $^{210}\text{Pb}$  in sediments of Lake St. Clair. *Can. J. Fish. Aquat. Sci.* **47**: 572–587.
- SCHAFFER, C. T., J. N. SMITH, AND R. COTÉ. 1990. The Saguenay Fjord: A major tributary to the St. Lawrence Estuary. *Coastal and Estuarine Studies*, 39, p. 378–420. *In* M. El-Sabh and N. Silverberg [eds.], *Oceanography of a large scale estuarine system, the St. Lawrence*. Springer-Verlag.
- , ———, AND D. H. LORING. 1980. Recent sedimentation events at the head of the Saguenay Fjord. *Environ. Geology* **3**: 139–150.
- SILVERBERG, N. NGUYEN, H. V., G. DELIBRIAS, M. KOIDE, B. SUNDBY, Y. YOKOYAMA, AND R. CHESSELET. 1986. Radionuclide profiles, sedimentation rates and bioturbation in modern sediments of the Laurentian Trough, Gulf of St. Lawrence. *Oceanol. Acta* **9**: 285–290.
- , AND B. SUNDBY. 1990. Sediment–water interaction and early diagenesis in the Laurentian Trough. *Coastal and Estuarine Studies*, 39, p. 202–238. *In* M. El-Sabh and N. Silverberg [eds.], *Oceanography of a large scale estuarine system, the St. Lawrence*. Springer-Verlag.
- SMITH, J. N. 1988. Pollution history and paleoclimatic signals in sediments of the Saguenay Fjord. *In* P. M. Strain [ed.], *Chemical oceanography in the Gulf of St. Lawrence*. *Can. Bull. Fish. Aquat. Sci.* **220**: 123–138.
- , AND K. M. ELLIS. 1982. Transport mechanism for Pb-210, Cs-137 and Pu fallout radionuclides through fluvial-marine systems. *Geochim. Cosmochim. Acta* **46**: 941–954.
- , ———, K. NAES, S. DAHLE, AND D. MATISHOV. 1995. Sedimentation and mixing rates of fallout radionuclides in Barents Sea sediments off Novaya Zemlya. *Deep-Sea Res. II* **42/6**: 1471–1493.
- , ———, AND D. M. NELSON. 1987. Time-dependent modelling of fallout radionuclide transport through a drainage basin; significance of “slow” erosional and “fast” hydrological components. *Chem. Geol.* **63**: 157–180.
- , AND D. H. LORING. 1981. Geochronology for mercury pollution in the sediments of the Saguenay Fjord. *Environ. Sci. Technol.* **15**: 944–951.
- , AND A. WALTON. 1980. Sediment accumulation rates and geochronologies measured in the Saguenay Fjord using the  $^{210}\text{Pb}$  dating method. *Geochim. Cosmochim. Acta* **44**: 225–240.
- STRAIN, P. M. 1988. Chemical oceanography in the Gulf of St. Lawrence: Geographic, physical oceanographic and geologic setting. *In* P. M. Strain, [ed.], *Chemical oceanography in the Gulf of St. Lawrence*. *Can. Bull. Fish. Aquat. Sci.* **220**: 1–14.
- SUNDBY, B. 1974. Distribution and transport of suspended particulate matter in the Gulf of St. Lawrence. *Can. J. Earth Sci.* **11**: 1517–1533.
- SYVITSKI, J. P., AND D. B. PRAEG. 1989. Quaternary sedimentation in the St. Lawrence Estuary and adjoining areas, Eastern Canada: An overview based on high resolution seismo-stratigraphy. *Geogr. Phys. Quat.* **43**: 291–310.
- , J. N. SMITH, E. A. CALABRESE, AND B. P. BOUDREAU. 1988. Basin sedimentation and the growth of prograding deltas. *J. Geophys. Res.* **93**: C6, 6895–6908.
- WHITE, C. 1994. Étude des gradients biogéochimiques entourant les tubes de polychètes dans les sédiments du chenal Laurentien. M.Sc. thesis, Univ. du Québec-Rimouski.
- YEATS, P. A. 1988. Distribution and transport of suspended particulate matter. *In* P. M. Strain [ed.], *Chemical oceanography in the Gulf of St. Lawrence*. *Can. Bull. Fish. Aquat. Sci.* **220**: 15–28.
- . 1990. Reactivity and transport of nutrients and metals in the St. Lawrence Estuary. *Coastal and Estuarine Studies*, 39, p. 109–129. *In* M. El-Sabh and N. Silverberg [eds.], *Oceanography of a large scale estuarine system, the St. Lawrence*. Springer-Verlag.

Received: 22 August 1995

Accepted: 11 March 1998

Amended: 8 September 1998